Silicon (2022) 14:1–11
https://doi.org/10.1007/s12633-020-00757-y

ORIGINAL PAPER

Effect of SiC Content on Mechanical and Tribological Properties of Al2024-SiC Composites

Dipankar Dey[1] · Abhijit Bhowmik[1] · Ajay Biswas[1]

Received: 16 June 2020 / Accepted: 5 October 2020 / Published online: 28 October 2020

Abstract

Aluminium matrix composites are scientifically engineered materials possessing higher potential in automotive, aerospace and defence applications. Therefore this study focuses on the fabrication of aluminium matrix composites reinforced with micro SiC particulates by stir casting process and investigating the effect of SiC content on mechanical properties as well as wear behaviour of the prepared composites. Different weight percentages (wt.%) of silicon carbide particulates (0, 3, 6 and 9%) were used. Stirring speed, time and other parameters were kept constant during the casting process. Microstructural characterization, tensile, hardness and wear tests were carried out of the casted samples. XRD analysis depicted the existence of SiC particulates in the prepared composites. Microstructural analysis confirms even distribution of reinforcement particulates. The experimental results revealed that, strength and hardness of the prepared composites improved with SiC addition. Wear resistance of SiC reinforced composites were also higher than that of the matrix alloy. The wear mechanism of matrix alloy was adhesive, whereas the wear mechanism changed to abrasive in case of SiC reinforced composites. The prepared composites exhibit augmented mechanical and tribological properties and can be used as a promising material in applications such as gears, drive shafts, brake drums and bearings.

Keywords Al2024 · SiC · Stir casting · Mechanical properties · Tribological properties

1 Introduction

Aluminium matrix composites (AMCs) are extensively employed in different industries as they offer high strength, wear resistance, corrosion resistance and thermal stability compared to monolithic materials [1]. Aluminium alloy 2024 introduced in the year 1931 possess good machining characteristics, fatigue resistance, high strength and high hardness; and is extensively used in aircrafts and automobiles. But Al2024 possess low tribological properties and hence there is a requirement of developing a composite having better wear resistance without negotiating the strength [2]. Fabrication of AMC is a challenging task in terms of homogeneity in reinforcement distribution. There are many processes adopted for AMC fabrication like stir casting, powder metallurgy, squeeze casting, diffusion bonding and friction stir processing. Among them, stir casting is one of the most efficient and economical process used for AMC fabrication. In stir casting process, reinforcement particles are mixed with molten metal with the help of mechanical stirring [3].

SiC [4, 5], Al_2O_3 [6], TiB_2 [7], Si_3N_4 [8], Fly Ash [9], B_4C [10] and Gr [11] are often used as reinforcements. Among them, SiC is one of the best suited reinforcement for AMCs, as it boosts up the strength, thermal stability and wear resistance [12]. AMCs fabricated with smaller particle size of SiC (4.7 μm) exhibits greater tensile strength and yield strength compared to larger particle size (77 μm). For smaller particles, tensile failure tend to "pull out" whereas AMCs fabricated with larger SiC particles, fractures easily [13]. Aluminium matrix composite reinforced with SiC exhibits an increase in hardness and density linearly with increment in the particle content. With the incorporation of SiC particles wear properties also enhanced significantly [14]. Artificially aged Al2024 alloy/SiC composite showed an enhancement in fatigue limit up to 100% by the inclusion of 5 wt.% SiCp. Further, incorporation of SiCp refines structure and also enhances the yield strength and elastic modulus [15]. Wear resistance capacity of

✉ Dipankar Dey
deybulton@gmail.com

[1] Mechanical Engineering Department, NIT Agartala, Tripura 799046, India

Fly Ash and SiC reinforced aluminium matrix composite increased significantly but wear rate increased with increment in distance and load. ANOVA results depicts that, wear rate of the hybrid composites was mostly influenced by load [16]. Tensile strength and hardness of Al2024/SiC composite increased remarkably by heat treatment [17]. Al–Si–Fe/SiC composite produced by stir casting, exhibits an increment in hardness and tensile strength followed by reduction in density and percentage elongation [18]. AA6061/SiC composites synthesized by stir casting process, exhibited an increment in density as well as hardness, with slight reduction in ductility with increment in the weight percentage of SiCp [19]. Stir casted AA6082/SiC/Gr hybrid composites exhibited an increment in hardness and strength with the inclusion of SiC and Gr particles [20]. The corrosive wear resistance of Al/SiC nanocomposites fabricated by mechanical milling increased significantly [21]. With the incorporation of nano SiCp to A356 alloy, the yield strength, elastic modulus and tensile strength of the composites improved but ductility reduced. The optimum mechanical behaviour was achieved by AMC reinforced with 3.5% SiC [22]. Tensile strength of (5%ABOw+15%SiCp)/6061Al composite enhanced with reduction in stirring temperature and increment in stirring time. Remarkable mechanical properties were achieved at stirring temperature of 640 °C and stirring time of 30 min [23]. Reinforcement volume fraction and size are the two major parameters influencing AMCs. High reinforcement volume fraction and smaller particles size together contributes towards strength enhancement of AMCs [24].

In summary, smaller particle size and higher volume fraction of SiCp in Al/SiC composites leads to enhancement in mechanical properties such as hardness and tensile strength, with reduction in ductility. However excessive increment in the volume fraction of SiCp leads to degradation of mechanical properties [25]. By the incorporation of high volume fraction of ceramic reinforcements, density of the composites also gets increased. Fabrication of Al/SiC composites becomes a challenging part on the researchers without negotiating the positive effect of ceramic reinforcements [26]. The present work aims at the development of Al2024-SiC composites by varying the wt.% of SiC particles using stir casting technique. Microstructure, ultimate tensile strength, density, porosity, hardness and wear behaviour of the fabricated composites were also investigated.

2 Experimental Details

Al2024 alloy was selected as the matrix. Table 1 illustrates the chemical composition of Al2024 alloy. Silicon carbide particulates having purity of 99.92% and size of 20 μm brought from Parshwamani Metals were used by varying the weight percentages (0, 3, 6 and 9%). During the trial experiments carried out with different higher weight percentages of SiC particulates, floating and clustering of reinforcement was observed and for avoiding the adverse effect of agglomeration of SiC particulates, the maximum wt.% of SiC addition was kept 9%. AMCs were fabricated by stir casting technique, with the help of a mechanical stirrer in an induction furnace (Fig. 1). At first Al2024 brought from Mallinath Metals, was cut into pieces of 700 g and melted in a graphite crucible at 700 °C. SiC powders were preheated in a separate muffle furnace at 450 °C for 30 min to remove the moisture content present within it. Then the powders were poured into the molten metal in a controlled manner. 2% magnesium was also added to the mixture for enhancing the wettability. Then the mixture was stirred continually at 350 rpm for 10 min with the aid of a mechanical stirrer to obtain sameness of the mixture. After proper mixing, the molten metal was poured into a preheated permanent mould and left for cooling to ambient temperature. The solidified metal was then removed from the mould and machined correctly for further analysis. Flow chart of the fabrication process is presented in Fig. 2.

Table 1 Chemical composition of Al2024 alloy

Element	Fe	Si	Mg	Mn	Cu	Zn	Ti	Cr	Al
wt.%	0.5	0.5	1.5	0.8	4.1	0.25	0.15	0.1	Bal.

XRD patterns of the prepared composites were obtained using Bruker D8 Advanced diffractometer with Cu-Kα radiation (Wavelength = 1.54178°A) and 2θ range from 10° to 70°. Microstructural characterizations were performed employing optical microscope (OM) and field emission scanning electron microscope with EDS (Model - Sigma 300, Carl Zeiss). Samples for microstructural analysis were first polished with emery papers of different grades and then with velvet cloth and alumina powder.

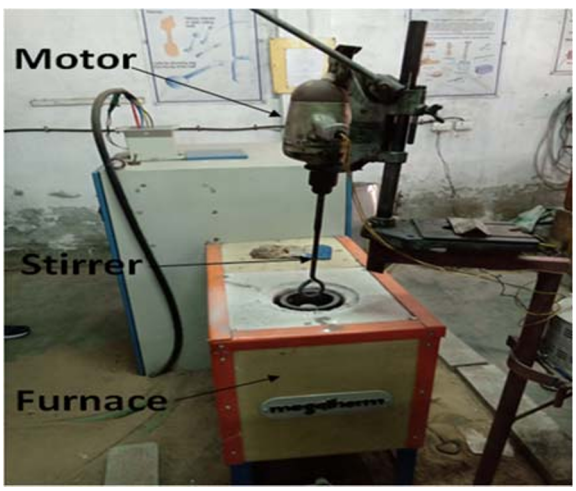

Fig. 1 Stir casting setup

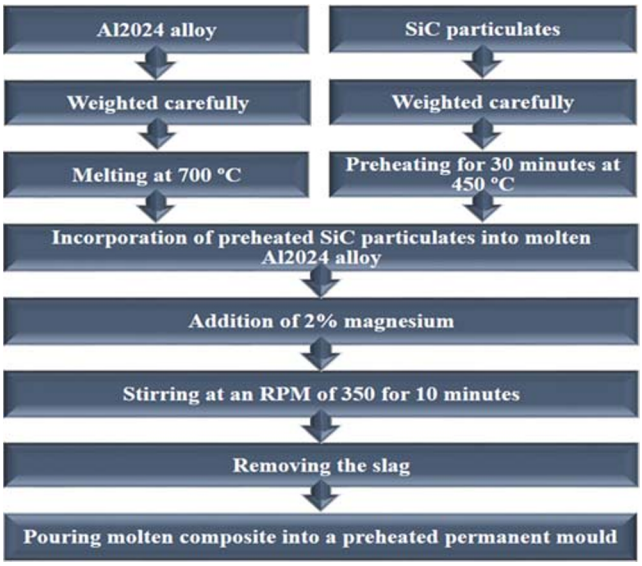

Fig. 2 Flow chart of the fabrication process

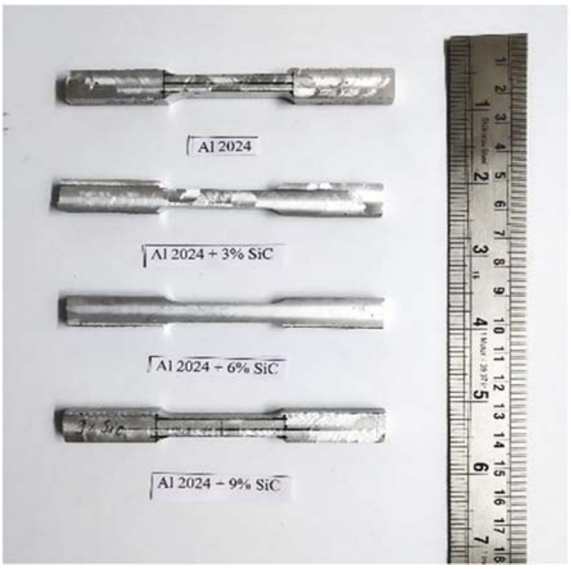

Fig. 3 Tensile specimens according to ASTM E8 standard

Density values of the prepared composites were obtained by Archimedes principle using a SAB-224CL density meter. Theoretical densities were determined by applying the rule of mixtures according to reinforcement weight percentage. Porosity values of the fabricated composites were determined by comparing the measured density with the theoretical density of every sample.

Rockwell hardness testing machine was used to determine hardness of the prepared composites with a loading of 100 kgf applied for 10 s. The Rockwell B-scale test was used for hardness characterization as it is commonly applied for determining the hardness of Al alloys. Hardness tests were performed for investigating the effect of reinforcement wt.% on hardness of the fabricated composites. In order to minimize variation in the hardness results, the actual hardness of each composite was taken as an average of ten measurements.

Tensile tests of the prepared composites were performed using a universal testing machine (HEICO HLC 693–35) with a crosshead speed of 0.5 mm/min. Tensile specimens were prepared according to ASTM E8 standard having 25 mm gauge length, 6 mm thickness and 6 mm gauge width (Fig. 3). An average of three tests was taken as the actual tensile result of each composite for minimizing uncertainty in the results.

Dry sliding wear tests were performed on a pin on disc tribotester (Model: Ducom TR 20LE-M5) at room temperature (Fig. 4). Cylindrical pins of length 40 mm and diameter 6 mm were prepared from all the casted composites and all the sliding faces of pins were polished with 400, 600 and 1000 grit emery papers respectively, for achieving uniformity in surface roughness and then cleaned with acetone. The tests were conducted by sliding the cylindrical pins against a hardened steel disc of EN31 material with hardness of 62 HRC. Prior to every testing, the counter disc was also polished with emery paper to get a smooth surface and lastly cleaned with acetone to clear away the footprint of foreign materials. The experiments were performed at various loads (10, 20 and 30 N), keeping the sliding distance and speed constant at 2000 m and 300 rpm respectively. The volume loss was determined after every experiment. For minimizing uncertainty in the experimental results, an average of three tests was taken as the actual result.

3 Results and Discussion

3.1 XRD Analysis

XRD patterns of the prepared Al2024-SiC composites are shown in Fig. 5. Peaks of silicon carbide (SiC) are present in

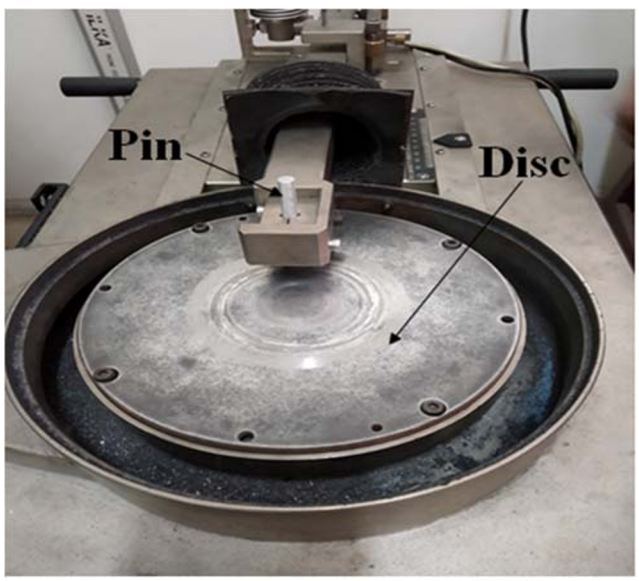

Fig. 4 Pin On Disc Tribotester

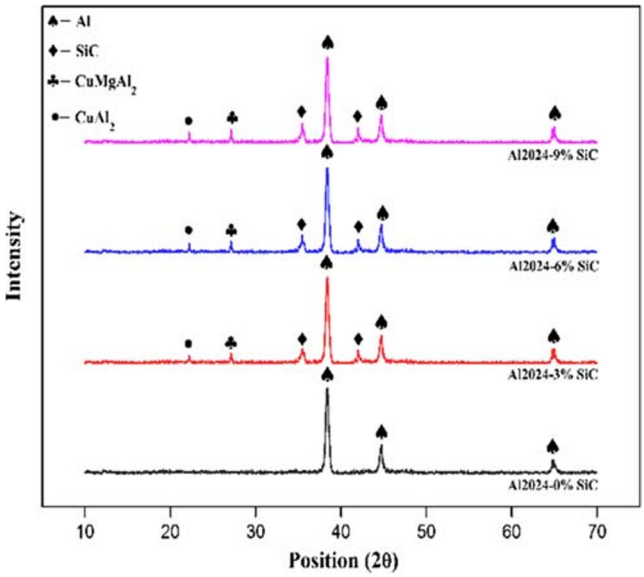

Fig. 5 XRD patterns of the prepared Al2024-SiC composites

the XRD patterns of SiC reinforced composites, which confirms the existence of SiC within the casted Al2024-SiC composites. Other compounds like $CuAl_2$ and $CuMgAl_2$ were also detected in the XRD analysis. No oxide peaks were detected in any of the XRD patterns of the prepared composites. Non-existence of oxide peaks confirms the achievement of excellent quality of casting.

3.2 EDS Analysis

The EDS spectrums of Al2024-SiC composites are shown in Fig. 6. Peaks of Si and C were detected in the spectrums (Fig. 6(b)-(d)), which confirms the existence of SiC in Al2024–3% SiC, Al2024–6% SiC and Al2024–9% SiC composites.

3.3 Microstructural Analysis

The optical micrographs of Al2024–6% SiC composite are presented in Fig. 7. From the optical micrographs, it can be seen that SiC particles are present and are distributed throughout the matrix. This distribution of SiC particulates can be attributed to optimum stirring parameters and incorporation of magnesium, which improves the wettability. For enhancing the mechanical and tribological properties of composites, homogeneity in reinforcement distribution is very important [27].

SEM micrographs of the prepared Al2024-SiC composites are presented in Fig. 8. Figure 8(a) shows the SEM image of the matrix alloy. Figure 8(b) depicts the existence of SiC particles in the prepared composite and it can also be observed that, Al2024–3% SiC composite is free from any casting defects, thus establishing an excellent matrix-reinforcement interfacial bonding. Some micro cracks and pores are present in Al2024–6% SiC composite (Fig. 8(c)). Existence of these pores can be ascribed to elevated viscosity of the melt [14]. But for higher reinforcement percentage, no cracks and pores were noticed. Figure 8(d) shows the SEM image of Al2024–9% SiC composite. It can be noted that clustering of reinforcement occurs when the reinforcement percentage increases. This clustering may result in non-uniformity in reinforcement distribution as well as degradation of mechanical and tribological properties of Al2024-SiC composites [28]. But the composite's performance has not deteriorated as can be seen from the hardness, tensile and wear tests, which shows higher mechanical properties and wear resistance capacity at 9 wt.% SiC. Moreover, literature suggests that clustering of reinforcement can enhance the composites strengthening mechanism when well bonded to the matrix [3].

3.4 Density and Porosity

Figure 9(a) shows the experimental and theoretical density profiles of the fabricated composites and it is evident that the theoretical and experimental density values closely matches with each other. Thus, it can be concluded that stir casting is well suited for successful composite preparation. From Fig. 9(a), it can also be observed that the density values of the prepared composites increases with increment in the wt.% of reinforcement. This increment in density values of Al2024-SiC composites can be attributed to the higher density of SiC particles compared to Al2024 alloy.

Figure 9(b) shows the porosity variation of the prepared composites with respect to reinforcement weight percentage. Porosity percentages of the fabricated composites increases with increment in the wt.% of reinforcement. This rise in porosity can be due to the incorporation of SiC into the matrix material or may be due to the existence of impurities within the composite. Porosity percentage of Al2024-SiC composites increased from 0.32% at 0 wt.% addition to 0.73% at 9 wt.% addition.

3.5 Hardness

Figure 10 shows the hardness of the fabricated composites with respect to weight percentage of reinforcement. From Fig. 10, it is evident that, an increasing trend of hardness has been observed with increment in the weight percentage of reinforcement. Hardness enhancement can be ascribed to the reality that, SiC possess higher hardness and its existence in the composite increases the hardness. Increment in hardness can also be associated with decreased grain size. Addition of silicon carbide into Al2024 alloy enhances the density of dislocation at the matrix-reinforcement interfaces. This enhancement in density of dislocation occurs because of the thermal

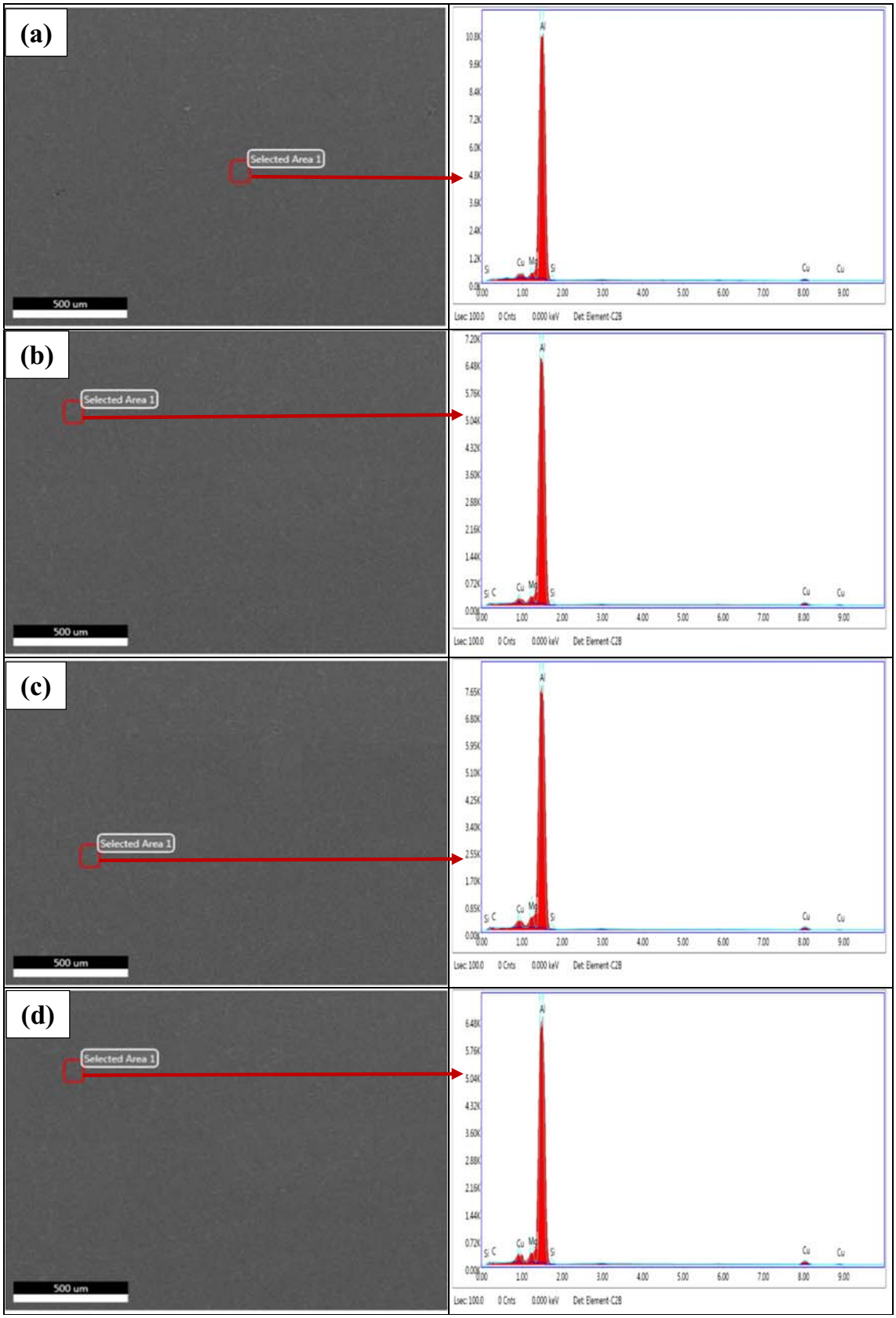

Fig. 6 EDS spectrums of (**a**) Al2024–0% SiC, **b** Al2024–3% SiC, **c** Al2024–6% SiC and **d** Al2024–9% SiC composites

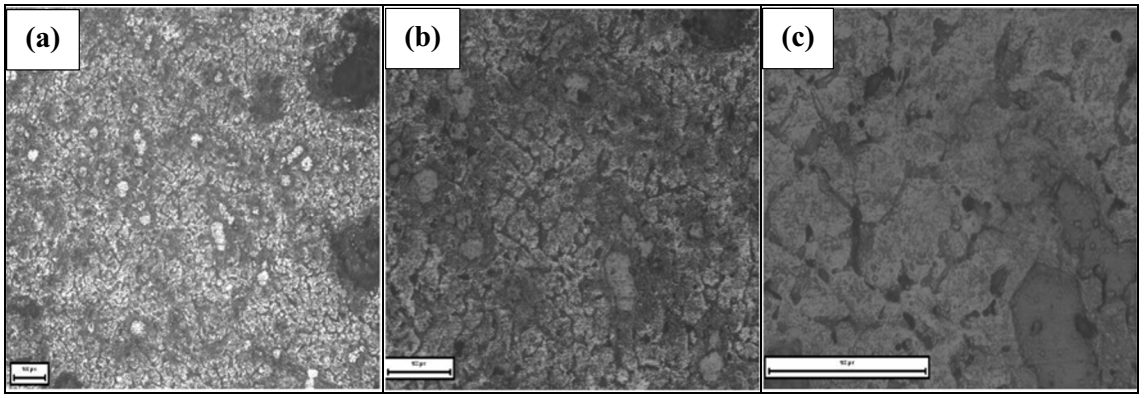

Fig. 7 Optical micrographs of Al2024–6% SiC composite; **a** 10X, **b** 20X and **c** 50X

expansion coefficient difference between the matrix and reinforcement, which results in increase in hardness [18]. Inclusion of magnesium increases wettability, which also boosts up the mechanical properties. Hardness of Al2024-SiC composites increased from 41.75 HRB at 0 wt.% addition to 55.7 HRB at 9 wt.% addition.

3.6 Tensile Strength

Figure 11 shows the tensile strength of the fabricated composites with respect to weight percentage of reinforcement. Results depict that, incorporation of silicon carbide particles into Al2024 alloy undoubtedly affects the tensile properties. Ultimate tensile strength of the fabricated composite significantly improved than the monolithic Al2024 alloy. It can be because of the fact that, fine SiC particles facilitates excellent interfacial bonding with the matrix material. Secondly, variation in thermal expansion coefficient also affects composites strengthening mechanism [29]. The thermal expansion coefficient of SiC is 4×10^{-6}/°C and Al2024 alloy is 24×10^{-6}/°C. This variation promotes high amount of dislocation all across the reinforcement particles at the time of solidification. Interaction among this dislocation and reinforcement particles enhances strength of the prepared composites. Rise in the

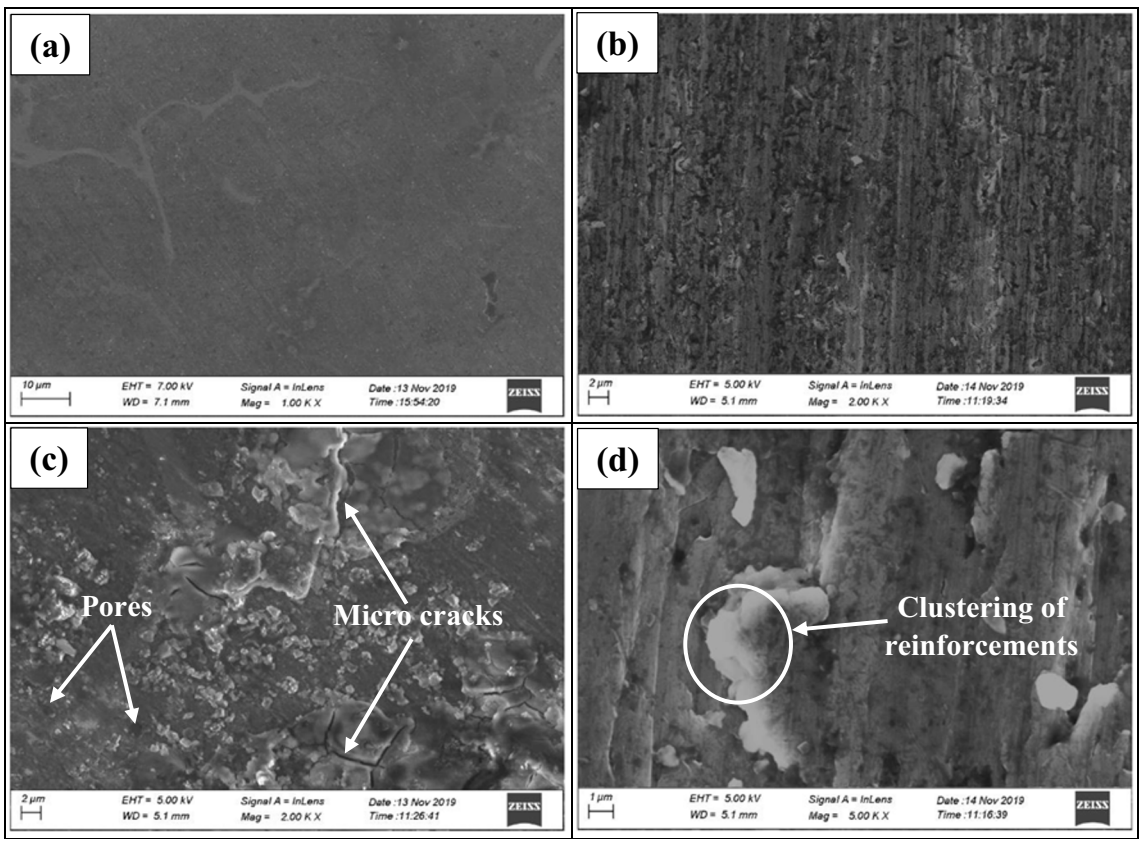

Fig. 8 SEM images of (**a**) Al2024–0% SiC, **b** Al2024–3% SiC, **c** Al2024–6% SiC and **d** Al2024–9% SiC (at higher magnification) composites

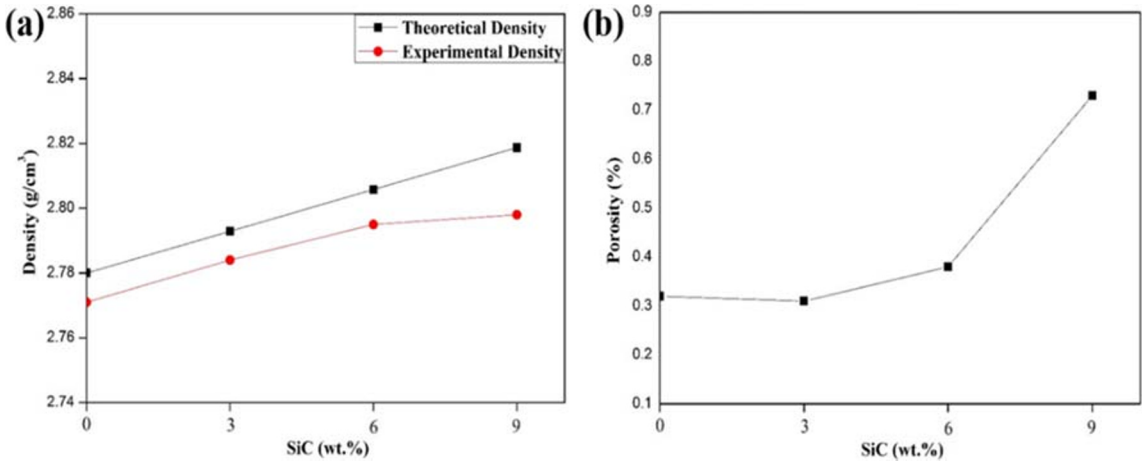

Fig. 9 Variation in (**a**) theoretical and experimental densities and (**b**) porosity percentages of Al2024-SiC composites with weight percentage of reinforcement

reinforcement wt.% also enhances this dislocation-reinforcement interaction thus increasing the strength. Ultimate tensile strength of Al2024-SiC composites increased from 188.61 N/mm^2 at 0 wt.% addition to 247.44 N/mm^2 at 9 wt.% addition.

Figure 12 displays the fracture surfaces of Al2024-SiC composites. From Fig. 12(a), it can be clearly seen that the fracture surface of matrix alloy consists of numerous dimples, which confirms the nature of failure to be purely ductile. But, the fracture surfaces of SiC reinforced composites comprises of dimples in the matrix phase and decohesion of reinforcement from the matrix phase (Fig. 12(b)-(d)). Occurrence of dimples can be attributed to nucleation of voids and coalescence caused by shear deformation and decohesion of reinforcement can be attributed to work-hardening and ceramic fragmentation caused by stress concentration [30]. Thus confirming the occurrence of both ductile as well as brittle fracture in case of SiC reinforced composites. It can be concluded that the addition of SiC leads to reduction in ductility [31].

3.7 Wear Behaviour

3.7.1 Effect of Reinforcement on Wear

Wear tests were performed with four different (0, 3, 6 and 9) wt.% of reinforcements. Figure 13 shows the impact of wt.% of reinforcement on volume loss of the prepared composites. It can be noted that the matrix alloy's volume loss at all load circumstances is more than the fabricated composites. From Fig. 13 it can also be noticed that, with increase in reinforcement wt.% volume loss decreases, which is due to the fact that, addition of SiC increases the hardness, as SiC forms a robust interfacial bond with the matrix material [16]. This hardness increment enhances the load bearing capacity which in turn augments the wear resistance capacity [32, 33].

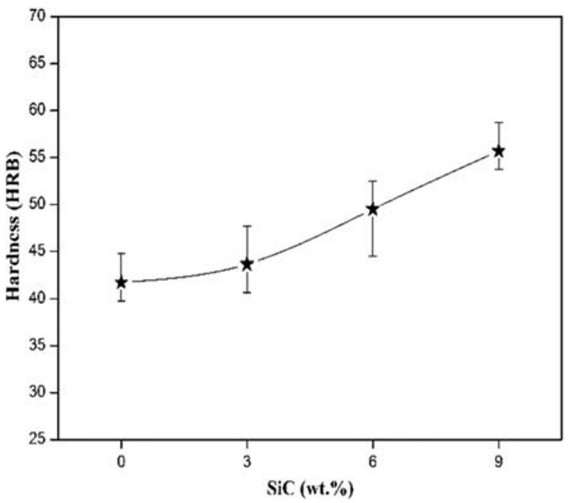

Fig. 10 Hardness of the fabricated composites with respect to weight percentage of reinforcement

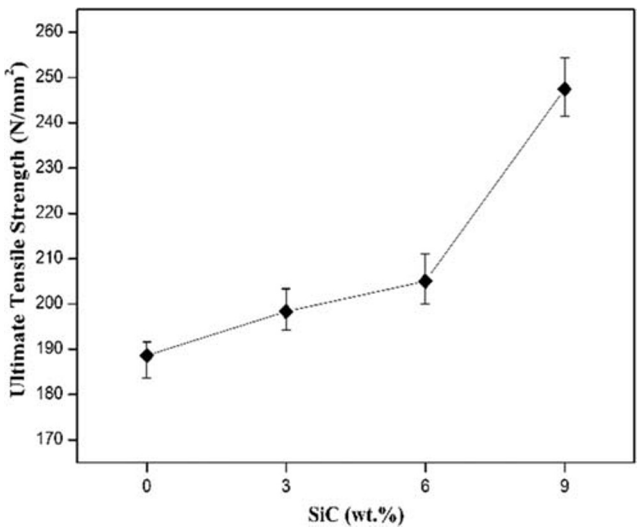

Fig. 11 Tensile strength of the fabricated composites with respect to weight percentage of reinforcement

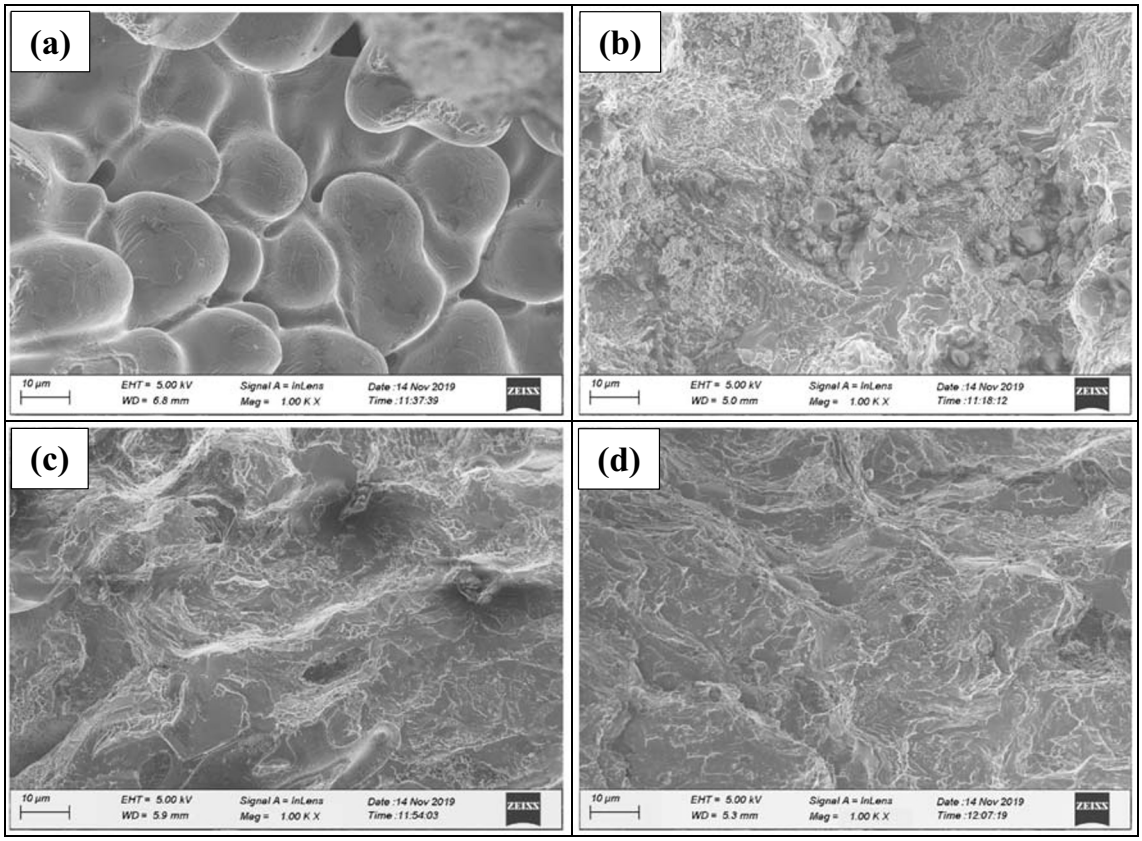

Fig. 12 Fracture surfaces of (**a**) Al2024–0% SiC, **b** Al2024–3% SiC, **c** Al2024–6% SiC and **d** Al2024–9% SiC composites

3.7.2 Effect of Applied Load on Wear

The wear tests were carried out by varying the loads (10, 20 and 30 N). Figure 14 represents the volume loss of the prepared composites as a function of load. Figure 14 reveals that, volume loss increases with increment in applied load. This is because, rise in applied load generates higher contact pressure and temperature. Due to this rise in surface temperature, plastic deformation of the pin surface causes the pin sliding face to adhere to the disc which ends up in higher material removal [16]. For same load, higher reinforced composite exhibits enhanced wear resistance than lower reinforced composite. But for same reinforced composite, wear rate increases with an increment in load. At higher loads of 30 N scratching and grooving appears to be more serious. This is because of abrasion, where hard asperities present between contact

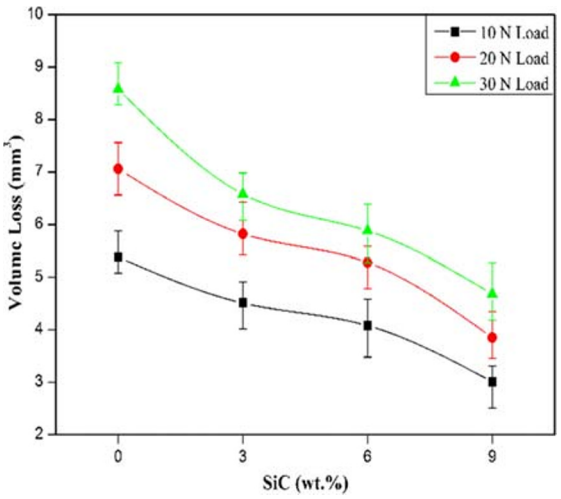

Fig. 13 Volume loss of the composites with respect to weight percentage of reinforcement

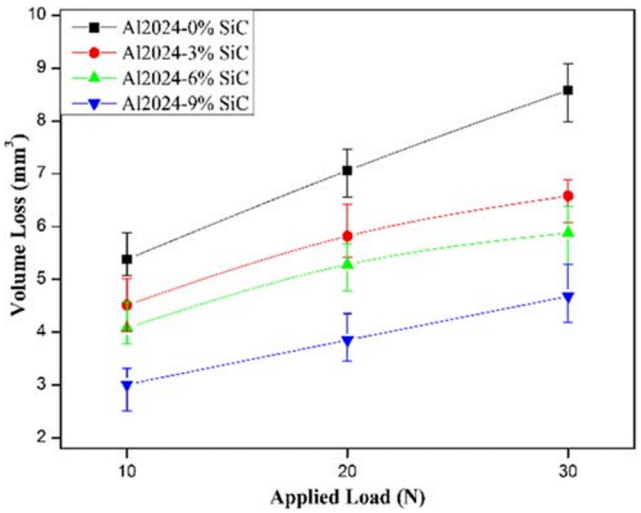

Fig. 14 Volume loss of the composites with respect to load

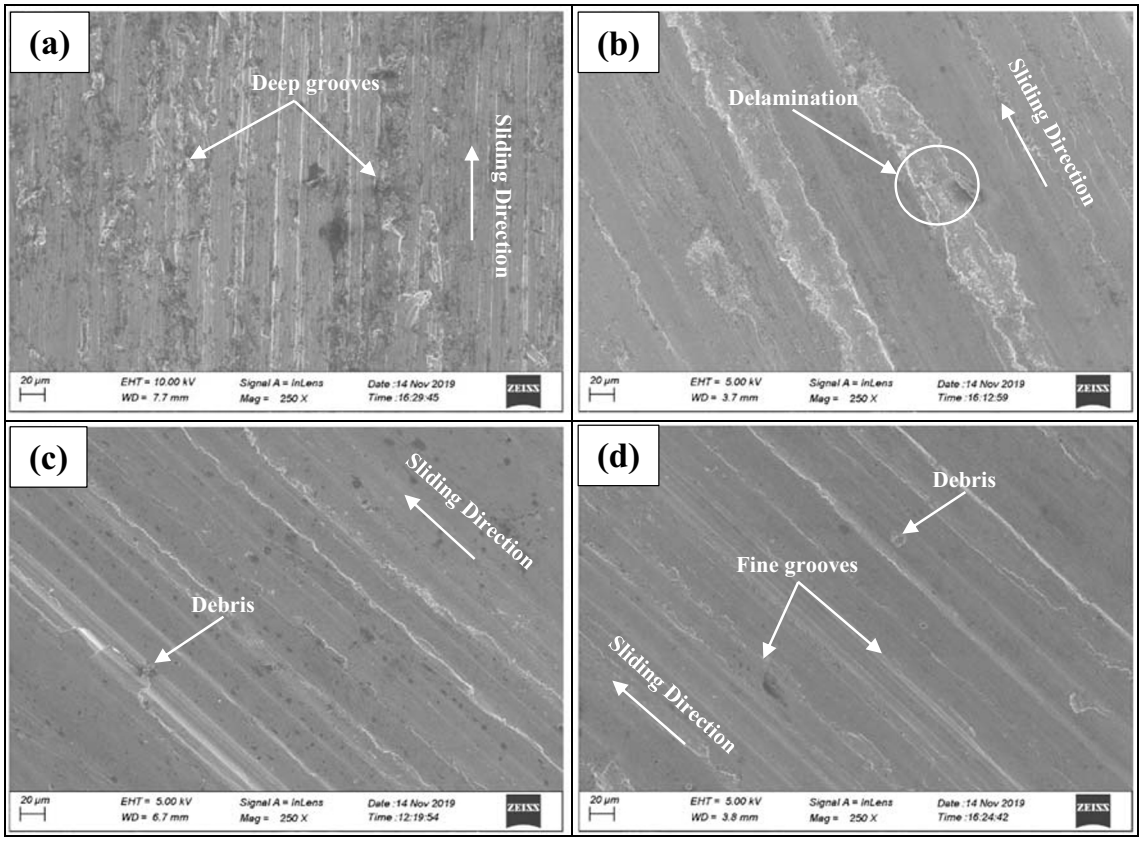

Fig. 15 Wear tracks of (**a**) Al2024–0% SiC, **b** Al2024–3% SiC, **c** Al2024–6% SiC and **d** Al2024–9% SiC composites at load 10 N

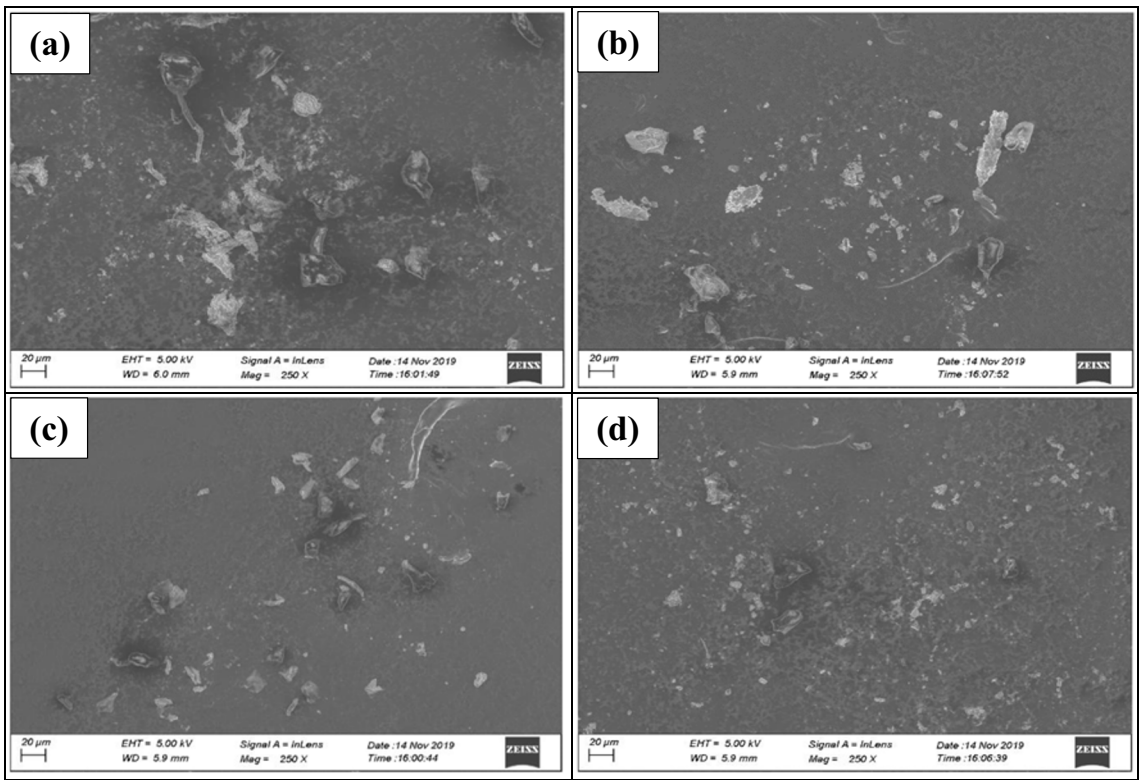

Fig. 16 Wear debris of (**a**) Al2024–0% SiC, **b** Al2024–3% SiC, **c** Al2024–6% SiC and **d** Al2024–9% SiC composites at load 10 N

surfaces, cut into the pin, resulting in scratching. Abrasion occurs mainly through ploughing, where material is displaced from either side of the groove without removal, which leads to wear out of small wedge-shaped fragments during contact with abrasive particles. Prolonged sliding causes sub-surface cracks that slowly develop and ultimately shear the surface, forming lengthy and thin sheets of wear. Delamination under high loads is noted to be higher [34]. Delamination includes deformation of the sub-surface, nucleation and propagation of cracks [35]. The relationship between applied load and volume loss can be best understood by the Archard's equation [36]:

$$V = kPL/H \tag{1}$$

where, V is the volume loss, k is a dimensionless constant, P is the applied load, L is the sliding distance and H is the hardness. From eq. (1) it can be noted that, volume loss is directly proportional to the applied load. Thus, it can be concluded that applied load is an important factor affecting the wear resistance.

Figure 15 displays the wear tracks of Al2024-SiC composites at load 10 N. The SEM micrograph of Al2024 alloy (Fig. 15(a)), shows some damaged regions which may lead to the generation of flake shaped debris. Figure 15(a) further depicts the existence of deeper grooves and severe plastic deformation thus resulting in enhancement in wear rate. Whereas, SiC reinforced composites exhibits finer grooves. Furthermore, size of these grooves goes on becoming finer with increment in the SiC content, thus confirming reduction in the severity of wear with the incorporation of SiC particles (Fig. 15(b)-(d)). All the SEM micrographs depicts the existence of wear debris on the worn surfaces, which indicates the occurrence of abrasive and adhesive wear during the wear tests.

Figure 16 shows the wear debris of Al2024-SiC composites at load 10 N. It can be seen that, flake shaped debris are generated from the unreinforced material (Fig. 16(a)), which can be because of the occurrence of severe damage during sliding. Whereas in case of SiC reinforced composites, smaller debris are produced (Fig. 16(b)-(d)). Furthermore, size of the wear debris continues to decrease with increment in the wt.% of SiC particles.

4 Conclusions

In this paper, the effect of SiC content on mechanical and tribological properties of Al2024-SiC composites was studied and the main conclusions are:

- Stir casting technique is one of the best suited techniques for the fabrication of Al2024-SiC composites.
- Uniform distribution of reinforcement was achieved (especially for lower wt.% of reinforcement) with good matrix-reinforcement bonding.
- Density and porosity values of the fabricated composites improved linearly with increment in the wt.% of reinforcement addition.
- Addition of SiC particulates enhances hardness of the prepared composites. Results reveal that AMC reinforced with 9 wt.% SiC was found to be the hardest with hardness of 55.7 HRB.
- Tensile strength of the fabricated composites increased with the addition of silicon carbide particulates.
- Volume loss of Al2024-SiC composites decreased significantly than the matrix material with the incorporation of SiC particles, whereas volume loss of the prepared composites increased with increase in applied load irrespective of SiC content.
- SEM micrographs of wear tracks revealed that the nature of wear mechanism was mild abrasive.
- Al2024–9% SiC composite can be used as a promising material in applications such as gears, drive shafts, brake drums and bearings.

References

1. Li PB, Chen TJ, Qin H (2016) Effects of mold temperature on the microstructure and tensile properties of SiC_p/2024 Al-based composites fabricated via powder thixoforming. Mater Des 112:34–45
2. Boopathi MM, Arulshri KP, Iyandurai N (2013) Evaluation of mechanical properties of aluminium alloy 2024 reinforced with silicon carbide and fly ash hybrid metal matrix composites. Am J Appl Sci 10(3):219–229
3. Singh G, Chan SLI, Sharma N (2018) Parametric study on the dry sliding wear behaviour of AA6082–T6/TiB_2 in situ composites using response surface methodology. J Braz Soc Mech Sci Eng 40(6):310
4. Dey D, Chintada SK, Bhowmik A, Biswas A (2020) Evaluation of wear performance of Al2024-SiC ex-situ composites. Materials Today: Proceedings 26:2996–2999. https://doi.org/10.1016/j.matpr.2020.02.619
5. Bahrami M, Helmi N, Dehghani K, Givi MKB (2014) Exploring the effects of SiC reinforcement incorporation on mechanical properties of friction stir welded 7075 aluminum alloy: fatigue life, impact energy, tensile strength. Mater Sci Eng A 595:173–178
6. Kök M (2006) Abrasive wear of Al_2O_3 particle reinforced 2024 aluminium alloy composites fabricated by vortex method. Compos A: Appl Sci Manuf 37(3):457–464
7. Dey D, Bhowmik A, Biswas A (2020) Wear behavior of stir casted aluminum-titanium diboride (Al2024-TiB_2) composite. Materials Today: Proceedings. 26:1203–1206. https://doi.org/10.1016/j.matpr.2020.02.242
8. Haq MIU, Anand A (2018) Dry sliding friction and wear behavior of AA7075-Si_3N_4 composite. Silicon 10(5):1819–1829
9. Manimaran R, Jayakumar I, Mohammad Giyahudeen R, Narayanan L (2018) Mechanical properties of fly ash composites—a review. Energy Sources, Part A: Recovery, Utilization, and Environmental Effects 40(8):887–893

10. Canakci A, Arslan F, Varol T (2013) Effect of volume fraction and size of B_4C particles on production and microstructure properties of B_4C reinforced aluminium alloy composites. Mater Sci Technol 29(8):954–960
11. Jinfeng L, Longtao J, Gaohui W, Shoufu T, Guoqin C (2009) Effect of graphite particle reinforcement on dry sliding wear of SiC/Gr/Al composites. Rare Metal Mater Eng 38(11):1894–1898
12. Bhandare RG, Sonawane PM (2013) Preparation of aluminium matrix composite by using stir casting method. International Journal of Engineering and Advanced Technology (IJEAT) 3(3): 61–65
13. Wang Z, Song M, Sun C, He Y (2011) Effects of particle size and distribution on the mechanical properties of SiC reinforced Al–Cu alloy composites. Mater Sci Eng A 528(3):1131–1137
14. Sahin Y, Acılar M (2003) Production and properties of SiCp-reinforced aluminium alloy composites. Compos A: Appl Sci Manuf 34(8):709–718
15. Bekheet NE, Gadelrab RM, Salah MF, El-Azim AA (2002) The effects of aging on the hardness and fatigue behavior of 2024 Al alloy/SiC composites. Mater Des 23(2):153–159
16. Kurapati VB, Kommineni R, Sundarrajan S (2018) Statistical analysis and mathematical modeling of dry sliding wear parameters of 2024 aluminium hybrid composites reinforced with fly ash and SiC particles. Trans Indian Inst Metals 71(7):1809–1825
17. Liu P, Wang A, Xie J, Hao S (2015) Effect of heat treatment on microstructure and mechanical properties of SiCp/2024 aluminum matrix composite. Journal of Wuhan University of Technology-Mater. Sci Ed 30(6):1229–1233
18. Aigbodion VS, Hassan SB (2007) Effects of silicon carbide reinforcement on microstructure and properties of cast Al–Si–Fe/SiC particulate composites. Mater Sci Eng A 447(1–2):355–360
19. Kumar GV, Rao CSP, Selvaraj N (2012) Studies on mechanical and dry sliding wear of Al6061–SiC composites. Compos Part B 43(3): 1185–1191
20. Sharma P, Paliwal K, Dabra V, Sharma S, Sharma N, Singh G (2018) Influence of silicon carbide/graphite addition on properties of AA6082 reinforced composites. Australian journal of mechanical engineering 1-9
21. Mosleh-Shirazi S, Akhlaghi F, Li DY (2016) Effect of SiC content on dry sliding wear, corrosion and corrosive wear of Al/SiC nanocomposites. Trans Nonferrous Metals Soc China 26(7):1801–1808. https://doi.org/10.1016/S1003-6326(16)64294-2
22. Mazahery A, Shabani MO (2012) Characterization of cast A356 alloy reinforced with nano SiC composites. Trans Nonferrous Metals Soc China 22(2):275–280
23. Guan LN, Lin G, Zhang HW, Huang LJ (2011) Effects of stirring parameters on microstructure and tensile properties of (ABO_w+SiC_p)/6061Al composites fabricated by semi-solid stirring technique. Trans Nonferrous Metals Soc China 21:s274–s279
24. Knowles AJ, Jiang X, Galano M, Audebert F (2014) Microstructure and mechanical properties of 6061 Al alloy based composites with SiC nanoparticles. J Alloys Compd 615:S401–S405
25. Ye T, Xu Y, Ren J (2019) Effects of SiC particle size on mechanical properties of SiC particle reinforced aluminum metal matrix composite. Mater Sci Eng A 753:146–155
26. Singh J, Chauhan A (2017) Fabrication characteristics and tensile strength of novel Al2024/SiC/red mud composites processed via stir casting route. Trans Nonferrous Metals Soc China 27(12): 2573–2586
27. El-Kady O, Fathy A (2014) Effect of SiC particle size on the physical and mechanical properties of extruded Al matrix nanocomposites. Mater Des 54:348–353
28. Erdemir F, Canakci A, Varol T (2015) Microstructural characterization and mechanical properties of functionally graded Al2024/SiC composites prepared by powder metallurgy techniques. Trans Nonferrous Metals Soc China 25(11):3569–3577
29. Mahamani A, Jayasree A, Mounika K, Prasad KR, Sakthivelan N (2015) Evaluation of mechanical properties of AA6061-TiB_2/ZrB_2 in-situ metal matrix composites fabricated by K_2TiF_6-KBF_4-K_2ZrF_6 reaction system. Int J Microstruct Mater Prop 10(3–4): 185–200
30. Min SONG (2009) Effects of volume fraction of SiC particles on mechanical properties of SiC/Al composites. Trans Nonferrous Metals Soc China 19(6):1400–1404
31. Allien VJ, Kumar H, Desai V (2019) Dynamic analysis and optimization of SiC reinforced Al6082 and Al7075 MMCs. Materials Research Express 6(5):056528
32. Singh N, Mir IUH, Raina A, Anand A, Kumar V, Sharma SM (2018) Synthesis and tribological investigation of Al-SiC based nano hybrid composite. Alexandria engineering journal 57(3): 1323–1330
33. Dey D, Biswas A (2020) Comparative study of physical, mechanical and Tribological properties of Al2024 alloy and SiC-TiB_2 composites. Silicon. https://doi.org/10.1007/s12633-020-00560-9
34. Haq MIU, Anand A (2018) Dry sliding friction and wear behaviour of hybrid AA7075/Si_3N_4/Gr self lubricating composites. Materials Research Express 5(6):066544
35. Rao JB, Rao DV, Prasad KS, Bhargava NRMR (2012) Dry sliding wear behaviour of fly ash particles reinforced AA 2024 composites. Mater Sci-Pol 30(3):204–211
36. Tjong SC, Lau KC (2000) Dry sliding wear of TiB_2 particle reinforced aluminium alloy composites. Mater Sci Technol 16(1):99–102